translation, bridge angle, O(6) rotations, and hydrogen bonds were nearly perfectly predicted by the packing analysis. This was reflected in a very low R index for the predicted structure even prior to refinement against x-ray data. The even lower R index obtained after x-ray refinement points out the degree of reliability that can be obtained with this refinement method.

It is also interesting to compare the results obtained in this study with the previously made prediction of the cellulose II structure which made use of a rigid chain packing method.[2] In the latter, a probable conformation of the chain was established by ϕ, ψ rotations and then packed into the unit cell without further refinement of the conformation. Only helix rotation and translation, as well as limited O(6) rotations, were allowed as variables. The results were only partially conclusive, in that antiparallel polarity was correctly predicted but a choice of optimum hydrogen bonding could not be made. In addition, the chain rotations were off by nearly 10° and chain translation was almost 0.5 Å in error. This illustrates very clearly the utility of stereochemical packing analysis with fully variable models. In this connection, it is also noteworthy that the relatively small deviations shown in Tables VIII and IX can be significant in terms of final structure analysis.

Acknowledgment. This work has been supported by the National Science Foundation Grant No. MPS7501560.

Supplementary Material Available: Tables I, V, and VI (6 pages). Ordering information is given on any current masthead page.

References and Notes

(1) R. H. Marchessault and A. Sarko, *Adv. Carbohydr. Chem.*, **22**, 421–482 (1967).
(2) A. Sarko and R. Muggli, *Macromolecules*, **7**, 486–494 (1974).
(3) K. H. Gardner and J. Blackwell, *Biopolymers*, **13**, 1975–2001 (1974).
(4) W. A. Sisson, *Contrib. Boyce Thompson Inst.*, **12**, 31–44 (1941).
(5) A. Sarko, *J. Appl. Polym. Sci., Appl. Polym. Symp.*, **28**, 729–742 (1976).
(6) H. D. Chanzy, "Structure of Fibrous Biopolymers", Colston Papers No. 26, E. D. T. Atkins and A. Keller, Ed., Butterworths, London, 1975, pp 417–434.
(7) P. Zugenmaier and A. Sarko, *Biopolymers*, in press.
(8) T. Bluhm and A. Sarko, to be published.
(9) W. T. Winter and A. Sarko, *Biopolymers*, **13**, 1447–1460 (1974).
(10) W. T. Winter and A. Sarko, *Biopolymers*, **13**, 1461–1482 (1974).
(11) F. J. Kolpak and J. Blackwell, *Macromolecules*, **8**, 563–564 (1975).
(12) R. E. Franklin and R. G. Gosling, *Acta Crystallogr.*, **6**, 678–685 (1953).
(13) S. Arnott and W. E. Scott, *J. Chem. Soc., Perkin Trans. 2*, 324–335, (1972).
(14) P. Zugenmaier and A. Sarko, *Acta Crystallogr., Sect. B*, **28**, 3158–3166 (1972).
(15) D. W. Jones, *J. Polym. Sci.*, **42**, 173–188 (1960).
(16) P. R. Sundararajan, Ph.D. Thesis, University of Madras, Madras, India, 1969; A. G. Walton and J. Blackwell. "Biopolymers", Academic Press, New York, N.Y., 1973, p 34.
(17) A. Sarko, J. Southwick, and J. Hayashi, the following paper in this issue.

Packing Analysis of Carbohydrates and Polysaccharides. 7. Crystal Structure of Cellulose III_I and Its Relationship to Other Cellulose Polymorphs

Anatole Sarko,* Jeffrey Southwick, and Jisuke Hayashi

Department of Chemistry, SUNNY College of Environmental Science and Forestry, Syracuse, New York 13210, and Department of Applied Chemistry, Faculty of Engineering, Hokkaido University, Sappora, Japan. *Received May 19, 1976*

ABSTRACT: The crystal structure of cellulose polymorph III_I, obtained by treatment of native ramie cellulose with liquid ammonia, was solved through a combined stereochemical structure refinement and x-ray diffraction analysis. The structure is based on a parallel packing of chains very similar to that of cellulose I. The characteristics of the structure include the same intramolecular O(5)–O(3′) and O(2)–O(6′) hydrogen bonds and C(3)–O(6) intermolecular ones that bond the chains into sheets in cellulose I. The liquid ammonia apparently shifts adjacent sheets relative to one another into a metastable, higher energy structure which reverts back to cellulose I upon heating in water. A very similar structure for cellulose III_{II}, obtained by liquid ammonia treatment of cellulose II, was also predicted by the stereochemical analysis. This structure is antiparallel as is cellulose II and it resembles the latter in chain conformation and hydrogen bonds, although again it is metastable in comparison with cellulose II. The weak odd-order meridional reflections observed in the diffractograms of cellulose III are correctly predicted by relaxing the strict $P2_1$ chain symmetry, particularly with respect to the rotation of hydroxymethyl groups. This is consistent with the presence of a small amount of substituent group rotational disorder in the structure of cellulose III. As was found to be the case with celluloses I and II, the stereochemical and x-ray refinement techniques complemented each other well and both were necessary in order to solve the structure.

Native crystalline cellulose, commonly known as cellulose I, gives rise to at least three polymorphic structures upon appropriate treatment.[1] For example, its regeneration or mercerization result in cellulose II, and both the latter as well as cellulose I can be converted to cellulose III through the use of liquid ammonia. Cellulose III, in turn, can be converted to cellulose IV by heat treatment. All four polymorphs crystallize well and their structures apparently differ only in the crystalline packing of chains with nearly the same conformation, because all four polymorphs show the same fiber repeat of ~10.3 Å.[1]

* SUNY College of Environmental Science and Forestry.

The highly crystalline cellulose I of the alga *Valonia ventricosa* has been previously shown to crystallize with a parallel packing of chains.[2,3] Whether the same is true for the less crystalline native celluloses of ramie, cotton, etc., is presently not known, but their x-ray diffraction patterns are nearly identical with that of *Valonia*, although less well resolved. Conversion of ramie or cotton celluloses into cellulose II results in a structure that is based on antiparallel packing of chains.[4,5] When, for example, ramie cellulose I or cellulose II are treated with liquid ammonia, two different cellulose III diffraction diagrams are obtained: the so-called III_I from cellulose I and the III_{II} from cellulose II.[6] Both are nearly, but

not completely, identical. Mild treatment, such as heating in water, reverts cellulose III_I back to cellulose I and cellulose III_{II} back to cellulose II. Previously, in a packing analysis of possible unit cells of cellulose, we had predicted that cellulose III could crystallize with either chain polarity but that both structures were less stable than celluloses I and II.[7] This is in keeping with the observed reversions.

In view of these observations and predictions, a determination of the crystalline structure of cellulose III_I became of interest. Initially, we attempted to convert cellulose I of *Valonia* into cellulose III_I, but this was not completely successful. Much better diffraction diagrams were obtained of ramie III_I and this sample thus became the primary source of x-ray diffraction data. The structure analysis was approached through combined stereochemical model analysis and x-ray diffraction intensity analysis, a method developed in this laboratory that has been successfully applied to other celluloses and polysaccharides.[4,8] As a part of this analysis, we also attempted to find an explanation for the well-known observation that cellulose III (among other polymorphs) exhibits weak odd-order meridional reflections, in apparent violation of the $P2_1$ space group, which is commonly presumed to apply to cellulose structures.

Experimental Section

Samples of cellulose III_I were prepared by treating fibers of ramie with liquid ammonia, using a procedure previously described.[6] Briefly, samples of ramie were immersed in liquid ammonia and kept at −80 °C for 20 h. The ammonia was then allowed to evaporate at −20 °C, making sure that the sample was not exposed to moisture in the process. The last traces of ammonia were removed by a stream of dry air at room temperature. The resulting cellulose III_I was then kept in a dry state in a desiccator over P_2O_5.

X-ray diffraction diagrams were obtained of small bundles of fibers in an evacuated Searle camera, with toroidally focussed Cu K_α radiation. The exposures were made on multiple sheet, flat-film packs of Ilford Type G Industrial X-Ray Film which was developed in freshly made Kodak Liquid X-Ray Developer at 20 °C. For the measurement of d spacings, the samples were dusted with finely powdered NaF crystals used as a calibrating standard. The reflection intensities were obtained by integration from radial tracings made with a Joyce-Loebl Mark IIIC Recording Densitometer. When two or more reflections appeared partly superimposed, intensities corresponding to each were obtained by computer least-squares resolution of the digitized intensity envelope.[9] Individual, integrated relative intensities thus obtained were corrected for Lorentz[10] and polarization factors, arcing of reflections, and unequal film-to-sample distances of diffracted rays and were then converted to relative structure amplitudes. The structure amplitudes of unobserved reflections were similarly determined by arbitrarily assigning to them one-half of the minimum observable intensity in the corresponding region of the diffraction angle.

The unit cell dimensions were obtained by computer least-squares fitting, using d spacings measured for single reflections with medium and above intensities.

Structure analysis and refinement was performed in two stages, with the first stage a stereochemical model analysis and the second an x-ray diffraction intensity analysis. The individual procedures are described in the Results and Discussion section.

All computations were performed with a CDC 3200 computer with 32K word memory.

Results and Discussion

X-Ray Measurements. A fiber diagram of ramie cellulose III_I is shown in Figure 1. Note that the 002 meridional is stronger than the 004 and that both 001 and 003 meridionals are weakly present. The d spacings of a total of 23 observed reflections could be measured and the resulting best fitting unit cell parameters were: a = 10.25 Å, b = 7.78 Å; c(fiber axis) = 10.34 Å; γ = 122.4°. The observed and calculated d spacings are listed in Table I.

The above unit cell compares well with others previously published[1] and for data obtained with both cellulose III_I and III_{II}.[11] The unit cell apparently remains the same regardless of the source of the polymorph. The unit cell volume dictates two chains per cell and even though a space group could not be unequivocally assigned, $P2_1$ would be likely if the weak odd-order meridionals were disregarded.

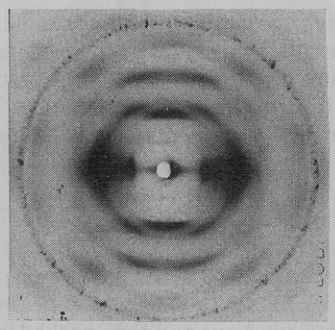

Figure 1. X-ray fiber diagram of cellulose III_I. Fiber axis is vertical.

Stereochemical Model Analysis. The methods and procedures of model analysis have been previously described in detail.[8] The first step was the choice of the most probable model for an isolated chain whose conformation was then refined against stereochemical criteria. As previously noted both in the analysis of the structure of cellulose I of *Valonia*[2] and the prediction of probable unit cells of cellulose polymorphs,[7] the most probable chain model is one with a twofold screw axis coincident with the chain axis. The screw axis may apply only to consecutive pyranose rings but not necessarily to their rotatable substituents. The helix parameters for such a model are n = 2 and h = 5.17 Å, and the ϕ, ψ rotational parameters[15] are ~145° and ~200°.[2] For a single chain with this backbone, three almost equally probable rotational positions of the hydroxymethyl group exist: gg, gt, and tg.[2] Of the three, tg is favored because it allows the formation of an O(2)–O(6′) intramolecular hydrogen bond, in addition to the O(5)–O(3′) bond present in all three models. The tg conformation exists in both chains of *Valonia* cellulose[2] and in one of the two chains of cellulose II.[4] Nevertheless, none of the above three chain models could a priori be eliminated and each was subjected to the next step in model analysis, the packing of chains into the unit cell.

Regardless of the chain model, the packing analysis of cellulose must consider both parallel and antiparallel packing polarities, because both are compatible with $P2_1$ or lower symmetries. The initial packing analysis was thus performed with six models: parallel chains with the hydroxymethyl groups in gt, gg, or tg positions, and the same for antiparallel chains. In initial analyses, all four hydroxymethyl groups present in the unit cell were considered to have the same rotational position. In subsequent analyses, each hydroxymethyl was allowed to rotate independently and mixed hydroxymethyl rotations were also included, e.g., tg for the corner chain and gt for the center chain, or alternating tg–gt sequences in the same chain. Similarly, in other analyses, the $P2_1$ symmetry was relaxed by allowing all four pyranose rings of the unit cell to rotate independently about their virtual bonds. (The latter is a vector connecting consecutive glycosidic oxygens.) This introduced up to four different bond angles at the glycosidic oxygens into the unit cell, two for each chain.

The chain packing analyses with variable hydroxymethyl and ring rotations were made partly in an attempt to account for the presence of the odd-order meridionals.

In all analyses, the starting atomic coordinate set was the average β-D-glucose residue, determined by Arnott and Scott by averaging known carbohydrate crystal structures.[12] The refinement of the packing of each model was conducted with methods and strategy that have previously been detailed.[8] In

Table II
Most Probable Models of Cellulose III_I Predicted by Packing Analysis

Model No.	O(6) position[a]	Bridge angle, deg	Chain rotations,[b] deg: Corner	Chain rotations,[b] deg: Center	Chain translation,[b] Å	Packing energy[c]	Hydrogen bonds and lengths,[d] Å	
			Parallel Chains					
1	tg (169°)	116	29	30	−2.57	18.1	$O(3)_{1-4}$–$O(6)_{1-4}$	2.62, 2.59
							O(5)–O(3′)	2.69
							O(2)–O(6′)	2.72
2	tg (161°, 162°) (168°, 170°)	115 117	30	24	−1.08	18.2	$O(3)_{1-4}$–$O(6)_{1-4}$	2.68, 2.67 2.66, 2.74
							O(5)–O(3′)	2.74, 2.65
							O(2)–O(6′)	2.77, 2.81
3	gt (40°)	115	36	35	−1.80	18.1	$O(2)_{1-4}$–$O(6)_{1-4}$	2.80, 2.90
							$O(3)_{1,2}$–$O(6)_{3,4}$	2.90
							$O(6)_{1,2}$–$O(2)_{3,4}$	2.73
							O(5)–O(3′)	2.76
4	gg (−60°)				Not possible			
5	tg, gt (170°) (41°)	116	30	32	−2.61	13.6	$O(3)_{1,2}$–$O(6)_{1,2}$	2.67
							$O(2)_{3,4}$–$O(6)_{3,4}$	2.84
							$O(3)_{1,2}$–$O(6)_{3,4}$	2.88
							O(5)–O(3′)	2.70
							O(2)–O(6′)	2.68
6	tg, gt alternating (168°, 45°) in same chain (169°, 40°)	116 117	29	26	−0.81	19.0	$O(3)_{1,3}$–$O(6)_{1,3}$	2.61, 2.57
							$O(2)_{2,4}$–$O(6)_{2,4}$	2.65, 2.76
							$O(2)_2$–$O(6)_4$	2.67
							$O(6)_2$–$O(2)_4$	2.57
							O(5)–O(3′)	2.64, 2.69
							O(2)–O(6′)	2.75, 2.82
			Antiparallel Chains					
7	tg (158°)	116	32	62	−3.41	17.8	$O(3)_{1-4}$–$O(6)_{1-4}$	2.71, 2.95
							$O(3)_{2,1}$–$O(6)_{3,4}$	2.78
							O(5)–O(3′)	2.78
							O(2)–O(6′)	2.80
8	gt (58°)	116	32	66	−3.92	30.7	O(2)–O(6)	2.53, 2.66
							O(5)–O(3′)	2.75
9	gg (−60°)				Not possible			
10	tg, gt (160°) (55°)	118 117	24	66	−1.91	12.5	$O(3)_{1,2}$–$O(6)_{1,2}$	2.67
							$O(2)_{3,4}$–$O(6)_{3,4}$	2.78
							$O(3)_{2,1}$–$O(6)_{3,4}$	2.78
							O(5)–O(3′)	2.70
							O(2)–O(6′)	2.96
11	tg, gt alternating (165°) in same chain (46°)	116	30	68	−2.43	14.2	$O(3)_1$–$O(6)_1$	2.57
							$O(2)_{2,4}$–$O(6)_{2,4}$	2.69, 2.82
							$O(2)_2$–$O(6)_3$	2.67
							$O(6)_2$–$O(3)_3$	2.81
							$O(6)_2$–$O(6)_4$	2.75
							O(5)–O(3′)	2.70
							O(2)–O(6′)	2.78

[a] O(6) is at 0° when the bond sequence O(5)–C(5)–C(6)–O(6) is cis. Rotation of C(6)–O(6) is positive clockwise looking from C(5) to C(6), and pure gt = 60°, tg = 180°, gg = −60°. [b] Corner chain 0° position is with $O(4)_1$ at 0, $-y$, z; for center chain with $O(4)_3$ at $a/2$, $b/2 - y$, z. Positive rotation is clockwise looking down the c axis. Translation is center chain relative to the corner chain along c. [c] The nonbonded portion of eq 1. [d] Atom subscripts indicate residue numbers: 1 and 2 for corner chain, 3 and 4 for center chain. Unsubscripted hydrogen bonds are intramolecular.

this method, all bond lengths, bond angles, and conformational angles were variable and the structure was refined by minimizing the arbitrary packing energy function:

$$Y = \sum_{i=1}^{l}\left(\frac{r_i - r_{0i}}{\mathrm{SD}_i{}^r}\right)^2 + \sum_{i=1}^{m}\left(\frac{\theta_i - \theta_{0i}}{\mathrm{SD}_i{}^\theta}\right)^2 + \sum_{i=1}^{n}\left(\frac{\phi_i - \phi_{0i}}{\mathrm{SD}_i{}^\phi}\right)^2 + \frac{1}{W^2}\sum_{i=1}^{N} w_{ij}(d_{ij} - d_{0ij})^2 \quad (1)$$

where r_i are bond lengths, θ_i the bond angles, ϕ_i the conformation angles, and d_{ij} the nonbonded distances. The corresponding standard values, r_{0i}, θ_{0i}, ϕ_{0i}, were obtained from known carbohydrate structures[12] and the standard d_{0ij} were previously determined by us from packing of carbohydrate crystal structures.[13]

The results of the stereochemical analysis are shown in Table II. For parallel packing, five equally probable models were found: two with the hydroxymethyl groups near the tg position (with one model of the two having unequal O(6) and ring rotations), one with O(6) near gt, and two with mixed tg and gt O(6). Similarly, for antiparallel packing, four models were found to be probable, but only three, one all tg and two mixed tg, gt O(6), were the most probable. Again, gg O(6) models were not possible.

All models showed good hydrogen bonding and an absence of short nonbonded contacts. It was therefore not possible to pick either the preferred polarity or the best O(6) model from the predicted structures. The final selection of the correct model thus fell on x-ray intensity analysis, as had been the case with *Valonia* cellulose I.

X-Ray Intensity Analysis. The starting models for the

Table III
X-Ray Intensity Refinement of Cellulose III_I Models

Model No.	O(6) position[a]	Bridge angle, deg	Chain rotations,[b] deg: Corner	Chain rotations,[b] deg: Center	Chain translation,[b] Å	R factor	Packing energy[c]	F_{002}/F_{004}	Temp factors[d]	Hydrogen bonds and lengths,[e] Å	
					Parallel Chains						
1	tg (172°)	116	31	33	−2.38	0.309	15.5	0.1	1.1	$O(3)_{1-4}$–$O(6)_{1-4}$	2.65, 2.56
									1.2	O(5)–O(3′)	2.73
									9.5	O(2)–O(6′)	2.66
2a	tg (177°, 169°)	116	31	25	−0.89	0.233	18.2	1.4	5.0	$O(3)_{1-4}$–$O(6)_{1-4}$	2.50, 2.69
	(169°, 164°)	117									2.68, 2.62
										O(5)–O(3′)	2.70, 2.68
											2.65, 2.67
										O(2)–O(6′)	2.77, 2.59
											2.84, 2.81
2b	tg (173°, 175°)	116	31	25	−0.90	0.205	17.0	1.4	5.9	$O(3)_{1-4}$–$O(6)_{1-4}$	2.59, 2.68
	(168°, 164°)	117							2.9		2.70, 2.64
									13.9	O(5)–O(3′)	2.66, 2.67
											2.69, 2.72
										O(2)–O(6′)	2.74, 2.60
											2.85, 2.82
3	gt (50°)	116	28	30	−0.98	0.299	36.7	1.5	5.0	$O(2)_{1-4}$–$O(6)_{1-4}$	2.97, 2.81
										$O(6)_{1,2}$–$O(2)_{3,4}$	2.36
										$O(3)_{1,2}$–$O(6)_{3,4}$	3.17
										O(5)–O(3′)	2.70
5	tg + gt (169°)	116	28	31	−2.69	0.270	16.0	0.4	5.8	$O(2)_{3,4}$–$O(6)_{3,4}$	2.76
	(44°)								0.5	$O(3)_{1,2}$–$O(6)_{1,2}$	2.68
									8.1	$O(3)_{1,2}$–$O(6)_{3,4}$	2.99
										O(5)–O(3′)	2.68
										O(2)–O(6′)	2.74
6	tg + gt alternating in (161°, 40°)	116	32	26	−0.88	0.251	25.1	1.8	5.0	$O(2)_{2,4}$–$O(6)_{2,4}$	2.40, 2.63
	same chain (161°, 48°)	117								$O(3)_{1,3}$–$O(6)_{1,3}$	2.48, 2.52
										$O(2)_2$–$O(6)_4$	2.95
										$O(6)_2$–$O(2)_4$	2.70
										O(5)–O(3′)	2.64, 2.67
											2.70
										O(2)–O(6′)	2.87, 2.97
					Antiparallel Chains						
7	tg (169°)	117	27	53	−2.81	0.322	26.4	0.6	5.0	$O(3)_{1-4}$–$O(6)_{1-4}$	2.64, 3.05
										O(5)–O(3′)	2.68
										O(2)–O(6′)	2.76
8	gt				Did not converge to a solution						
10a	tg + gt (167°, 168°)	117	29	63	−2.07	0.263	13.4	2.7	5.0	$O(3)_{1,2}$–$O(6)_{1,2}$	2.69, 2.63
	(67°, 66°)									$O(2)_{3,4}$–$O(6)_{3,4}$	2.62, 2.63
										$O(3)_{2,1}$–$O(6)_{3,4}$	2.78, 2.82
										O(5)–O(3′)	2.72
										O(2)–O(6′)	2.72, 2.76
10b	tg + gt (167°, 168°)	117	29	63	−2.07	0.205	13.4	2.7	7.0	$O(3)_{1,2}$–$O(6)_{1,2}$	2.69, 2.63
	(67°, 66°)								0.9	$O(2)_{3,4}$–$O(6)_{3,4}$	2.62, 2.63
									13.9	$O(3)_{2,1}$–$O(6)_{3,4}$	2.78, 2.82
										O(5)–O(3′)	2.72
										O(2)–O(6′)	2.72, 2.76
11	tg + gt alternating in (162°)	116	31	66	−2.93	0.332	18.0	0.1	5.0	$O(2)_{2,4}$–$O(6)_{2,4}$	2.72, 2.56
	same chain (54°)									$O(3)_1$–$O(6)_1$	2.56
										$O(2)_2$–$O(6)_3$	3.05
										$O(3)_2$–$O(6)_3$	2.80
										$O(6)_2$–$O(3)_3$	3.11
										$O(6)_2$–$O(6)_4$	2.62
										O(2)–O(6′)	2.82
										O(5)–O(3′)	2.72

[a] See footnote *a* in Table II. [b] See footnote *b* in Table II. [c] See footnote *c* in Table II. [d] Single temperature factor is isotropic; three values indicate the anisotropic temperature factors B_x, B_y, B_z of eq 3. [e] See footnote *d* in Table II.

structure refinement against x-ray intensities were the models shown in Table II, except those with O(6) gg. The same variable parameters were used as in stereochemical analysis and the success of refinement was measured by the minimization of the crystallographic disagreement index

$$R = \sum||F_o| - |F_c||/\sum|F_o| \quad (2)$$

where F_o and F_c are the observed and calculated structure amplitudes, respectively. In addition, anisotropic temperature factors B_x, B_y, and B_z given by the function

$$B = \frac{h^2a^{*2}}{4}B_x + \frac{k^2b^{*2}}{4}B_y + \frac{l^2c^{*2}}{4}B_z \quad (3)$$

(where hkl are reflection indices and a^*, b^*, c^* are reciprocal

Table V
Individual Ring Rotations, Bridge Angles, and O(6) Rotations for Models 2 and 6 of Table III (Calculated Meridional Structure Amplitudes for the Same Models)

Residue[a]	Ring rotation, deg (relative to residue 1)	Bridge angle, deg	O(6) rotation, deg	Calcd meridionals F_{001}	F_{002}	F_{003}	F_{004}
	Model 2, O(6) tg						
1	0	116.0	173	0.4	25.3	0.1	17.8
2	−3.8	116.1	175				
3	−5.9	116.8	168				
4	−4.1	116.7	164				
	Model 6, O(6) tg, gt						
1	0	116.2	161	11.9	29.9	10.0	16.3
2	0.5	116.4	40				
3	−4.8	117.1	161				
4	−5.9	117.2	48				

[a] Residues 1 and 2 are in the corner chain, 3 and 4 in the center chain.

lattice parameters) were included as refinement variables in the final stages. The procedure and strategy of x-ray refinement have also been previously detailed.[8] As an additional criterion, the meridional structure amplitudes were calculated for all refined models. The results of the analysis are shown in Table III.

When the three criteria of minimum R factor, correct ratio of meridional intensities, and the identity of the x-ray refined and stereochemically predicted structures are applied to the results shown in Table III, only two structures survive the tests: the parallel model number 2, with O(6) tg, and the antiparallel model number 10, with O(6) tg in the corner chain and gt in the center chain. Even though there is no clear-cut preference for either model, each of the above three criteria slightly favors the parallel model. For example, even though identical R factors of 0.205 are obtained for both models, individual experimental structure amplitudes of observed reflections compare better with the corresponding calculated quantities for the parallel model than for the antiparallel model (cf. Table IV). More importantly, the x-ray refined parallel structure is very close to that predicted by stereochemical analysis, showing differences of the order of one degree for chain rotations, less than 0.2 Å for chain translation and identical hydrogen bonds. For the antiparallel structure, these differences are somewhat larger, for example, up to 5° in chain rotation. The criterion of identity of the stereochemically and x-ray refined structures has previously been found to be an important one.[8]

Nonetheless, the preference for the parallel structure is slight and could be fortuitous, requiring, therefore, confirmation from other sources.

It is now well established that cellulose I of *Valonia* is a parallel chain structure.[2,3] Similarly definitive information on ramie cellulose I is not available, but there is no reason to suspect that the latter is different from *Valonia* in anything but crystalline perfection. Both experimental x-ray diffraction data and predictive analysis of cellulose unit cells are in agreement with this view. On the other hand, cellulose II has been conclusively shown to be an antiparallel structure.[4,5] Because there is no known way to convert antiparallel cellulose II into parallel I, and because the cellulose III_I of this study can be converted with ease back to cellulose I, it must be concluded that cellulose III_I is also a parallel structure.

It is interesting that the preferred III_I structure strongly resembles that of cellulose I, viz., both have all O(6) near the tg rotational position and both show the same hydrogen bonds. The latter bond the chains into sheets in two directions, by intramolecular O(5)–O(3′) and O(2)–O(6′) hydrogen bonds along the chain and by intermolecular O(3)–O(6) bonds in the lateral direction. The only differences between celluloses I and III_I thus reside in the relative positions of adjacent sheets.

The predicted antiparallel cellulose III structure also has a reasonable basis. It is known that a cellulose III_{II} can be prepared from cellulose II in the same manner as III_I is obtained from cellulose I.[6] The resulting structure has the same unit cell as III_I but shows a slightly different diffraction intensity distribution. It converts easily back to cellulose II. The cellulose II structure has a mixture of O(6) rotations, with the O(6)'s of the corner chain in the tg position and the O(6)'s of the center chain in the gt position.[4,5] The predicted antiparallel III structure is nearly identical with that of II in these respects, as well as in chain rotations and intersheet hydrogen bonds. The fact that a perfect correspondence between the stereochemically predicted and the x-ray refined structures was not obtained for the antiparallel model as it was for the parallel model simply reflects the use of the intensity data of III_I which are slightly different from those of III_{II}.

The appearance of odd-order meridionals in the diffraction diagrams of almost all cellulose polymorphs, and in particular cellulose III, has been a puzzle for a long time. A number of probable explanations have been offered, among them that the cellulose structure has no $P2_1$ symmetry and that the true repeat is a dimer rather than a monomer residue, and alternatively that the hydroxymethyl group rotations vary along the chain either in a systematic fashion or randomly. We attempted to test both hypotheses by removing first the $P2_1$ symmetry restriction on the chain backbone and then by allowing consecutive O(6) groups to alternate in tg, gt conformations. As previously indicated, the first restriction was removed simply by allowing all four monomer residues of the unit cell to rotate independently about their virtual bonds. This could result in all four bridge angles being different. But as shown in Table V, the virtual bond rotations varied little and the bridge angles remained nearly constant within the chain and varied only slightly between the corner and center chains. This did not result in the appearance of odd-order meridionals, as shown in Table V. On the other hand, as shown by model 6 in Table II, a parallel structure with an alternating sequence of tg and gt O(6) groups is a reasonable one and not far different from the most probable all tg structure. The virtual bond rotations and calculated meridionals for it are shown in Table V. It is clear that even a small percentage of such a mix of O(6) rotations will result in the observation of odd-order meridionals.

Finally, the hydrogen bonding sequences in the structure of cellulose III_I were determined by adding the heretofore not included hydroxyl hydrogens to the structure and allowing them to find their stereochemically most probable positions.

Table VI
Hydrogen Bond Lengths and Angles for the Scheme in Figure 2

Hydrogen bond[a]	Length, Å		Angles, deg[b]		
	O–O	O–H	θ_1	θ_2	θ_3
		Intramolecular			
$O(5)_1$–H-$O(3)_2$	2.72	2.44	21.5	95.2	63.3
$O(5)_2$–H-$O(3)_1$	2.69	2.20	20.6	108.5	50.9
$O(5)_3$–H-$O(3)_4$	2.65	2.11	20.5	111.8	47.7
$O(5)_4$–H-$O(3)_3$	2.67	2.23	21.2	105.0	53.8
$O(6)_2$–H-$O(2)_1$	2.63	1.92	36.5	125.5	18.0
$O(6)_1$–H-$O(2)_2$	2.60	2.18	54.7	103.4	21.9
$O(6)_4$–H-$O(2)_3$	2.85	2.05	28.7	137.7	13.6
$O(6)_3$–H-$O(2)_4$	2.82	2.05	32.6	132.1	15.3
		Intermolecular			
$O(3)_1$–H-$O(6)_1$	2.70	1.81	21.8	146.4	11.8
$O(3)_2$–H-$O(6)_2$	2.59	1.67	18.3	150.9	10.8
$O(3)_3$–H-$O(6)_3$	2.68	2.02	40.1	121.4	18.5
$O(3)_4$–H-$O(6)_4$	2.64	1.93	36.5	125.6	17.9

[a] Atom subscripts indicate residue numbers: 1 and 2 for corner chains as shown in Figure 2, 3 and 4 for the center chain in corresponding fashion. [b] Cf. Figure 2 for the description of angles.

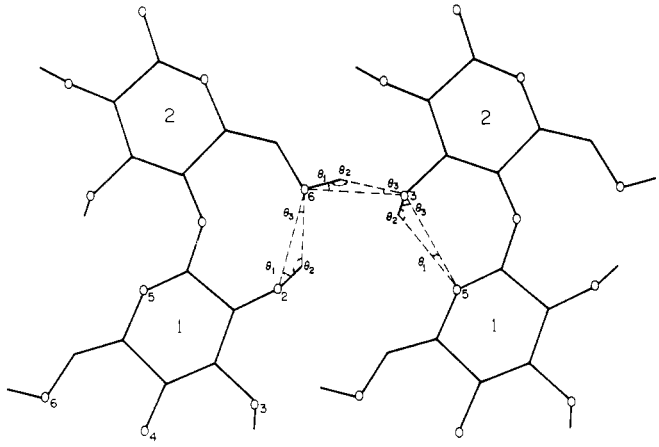

Figure 2. Hydrogen bond scheme of cellulose III_I shown between corner chains of the unit cell. The angles given in Table VI are indicated.

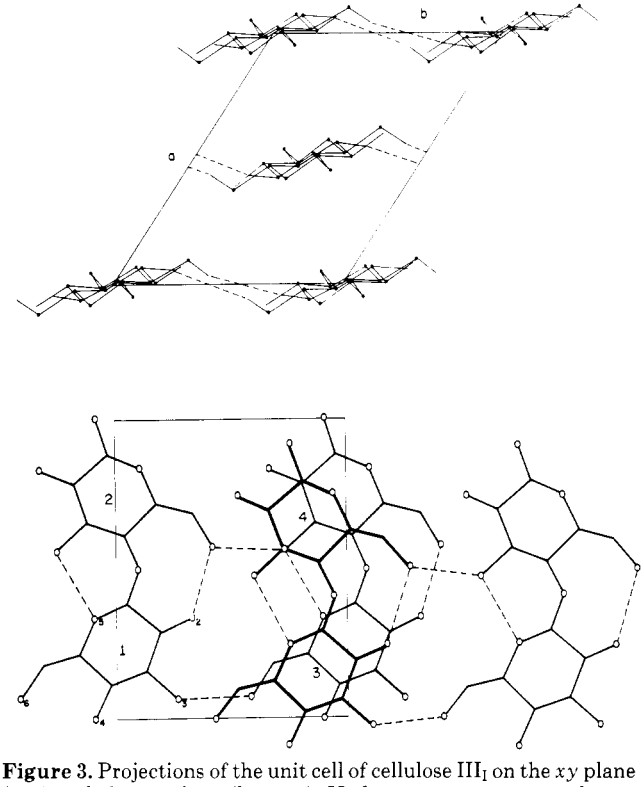

Figure 3. Projections of the unit cell of cellulose III_I on the xy plane (top) and the yz plane (bottom). Hydrogen atoms are not shown. Hydrogen bonds are shown as dashed lines between oxygen atoms.

The procedure for this step has been previously described in our structure analysis of cellulose II and involves, principally, the rotations of the three hydroxyl groups of each residue about the corresponding C–O bonds.[4] The resulting best hydrogen bond scheme is shown in Figure 2 and the corresponding bond length and angle data are given in Table VI. The addition of the hydroxyl hydrogens also dropped the R factor slightly, to 0.203.

The final crystal structure of cellulose III_I is shown in Figure 3 and the corresponding atomic coordinates are given in Table VII. The bond lengths, bond angles, and conformation angles of the refined structure are, without exception, within one standard deviation of the average values compiled from single crystal carbohydrate analyses.[12] Once again, this indicates the value of accurate stereochemical data as obtained from monomer and oligomer carbohydrate crystal structures. No short nonbonded contacts were found in this structure, except a slightly short interchain $O(3)_2$–$O(6)_2$ hydrogen bond at 2.59 Å.

Conclusions

The structure analysis of celluloses has always been difficult because the differences between various parallel and antiparallel packing models are small and not easily resolved by diffraction analysis. This is partly the reason why the crystal structures of cellulose polymorphs have remained unknown for such a long time. However, since the development of modern, computer-based stereochemical structure refinement techniques and their combination with diffraction analysis, the crystal structures of celluloses I, II, and now III_I have been solved in reasonable detail and with good accuracy. The coincidence of predicted and ultimately found structures has been very good and this lends confidence in the predictive aspects of the method as a tool for structure analysis where diffraction data are poor.

With these results, the relationships between and the interconversions of different cellulose polymorphs have now become clearer. Cellulose I, the native polymorph, is biosynthesized as a parallel chain structure, even though the latter

is a higher energy form relative to the antiparallel cellulose II. Presumably, the kinetics of biosynthesis are such that crystallization is either favored or faster than chain folding which otherwise would lead to an antiparallel structure. The chains crystallize into strongly hydrogen bonded sheets which lend cellulose its characteristic strength, yet the bonding between sheets is not strong, permitting structural flexibility necessary for plant cell walls and their growth. When a hydrogen bond breaker, such as ammonia, acts on cellulose I, all hydrogen bonds are probably broken and the structure rearranges into another least energy form that may be an ammonia complex. Because the cellulose chain is stiff and the ammonia treatment is not sufficiently drastic to solubilize the structure, chain folding does not occur in this complex. Upon evaporation of the ammonia, the cellulose structure reforms its intrasheet hydrogen bonds but settles into the nearest energy minimum which is cellulose III_I, retaining the parallel structure but showing a shift of sheets relative to the structure of cellulose I. Because the latter resides in a global minimum for parallel structures,[7] a supply of some energy to III_I results in its reversion to I. This process need not be a high energy one because hydrogen bond breaking is not needed in the shift of adjacent sheets. Although little is known about cellulose IV_I which can be made from III_I (or cellulose I) by high temperature heating in the solid state, the chances are good that it is also a parallel chain structure.

On the other hand, when cellulose I is solubilized and subsequently regenerated, the chains may fold[14] and seek out the true global minimum for cellulose crystal structures, the antiparallel cellulose II. The latter can also form an ammonia complex, because of the general similarity of parallel and antiparallel cellulose structures. This complex, however, results in an antiparallel cellulose III_{II} which is metastable with respect to II and reverts to the latter in the same fashion as III_I reverts to I. Again, on the strength of similarities in structures, there probably exists a IV_{II} which is antiparallel. Because the differences in the structures of III_I and III_{II} reside mainly in chain polarity, as is true of the structures of I and II, the solid state conversions of II to I and III_{II} to III_I cannot occur.

Acknowledgment. This study was supported by National Science Foundation Grant No. MP57501560.

Supplementary Material Available: Tables I, IV, and VII (5 pages). Ordering information can be found on any current masthead page.

References and Notes

(1) R. H. Marchessault and A. Sarko, *Adv. Carbohyd. Chem.*, **22**, 421–482 (1967).
(2) A. Sarko and R. Muggli, *Macromolecules* **7**, 486–494 (1974).
(3) K. H. Gardner and J. Blackwell, *Biopolymers*, **13**, 1975–2001, (1974).
(4) A. Stipanovic and A. Sarko, *Macromolecules*, preceding paper in this issue.
(5) F. J. Kolpak and J. Blackwell, *Macromolecules*, **8**, 563–564 (1975).
(6) J. Hayashi, A. Sufoka, J. Ohkita, and S. Watanabe, *Polym. Lett.*, **13**, 23–27 (1975).
(7) A. Sarko, *J. Appl. Polym. Sci., Appl. Polym. Symp.*, **28**, 729–742 (1976).
(8) P. Zugenmaier and A. Sarko, *Biopolymers*, in press.
(9) R. D. B. Fraser and E. Suzuki, *Anal. Chem.*, **38**, 1770–1773 (1966).
(10) R. E. Franklin and R. G. Gosling, *Acta Crystallogr.*, **6**, 678–685 (1953).
(11) H. J. Willard, *J. Polym. Sci.*, **13**, 474–476 (1954).
(12) S. Arnott and W. E. Scott, *J. Chem. Soc., Perkin Trans. 2*, 324–335 (1972).
(13) P. Zugenmaier and A. Sarko, *Acta Crystallogr., Sect. B*, **28**, 3158–3166 (1972).
(14) H. D. Chanzy, "Structure of Fibrous Biopolymers", Colston Papers No. 26, E. D. T. Atkins and A. Keller, Ed., Butterworths, London, 1973, pp 417–434.
(15) The ϕ,ψ angles are measured according to the convention used in ref 2.

Notes

Comments on the Liquid State Conformations of *n*-Alkanes

ALAN E. TONELLI

Bell Laboratories, Murray Hill, New Jersey 07974.
Received January 19, 1976

Recently Champion and co-workers,[1,2] in attempting to account for molecular weight anomalies observed in their flow birefringence and laser light-scattering studies of liquid *n*-alkanes, proposed that an abrupt change in the conformational characteristics occurs between the C_{12} and C_{14} members of this homologous series of liquids. To explain the differences in the temperature dependence of the flow birefringence[1] and the low frequency depolarized spectra of scattered light[2] they observed between the smaller ($\leq C_{12}$) and larger ($\geq C_{14}$) *n*-alkane liquids, Champion and co-workers suggested[1,2] that the C_{12} and lower members exist predominantly in the all-trans, planar zigzag conformation, while the C_{14} and higher homologues experience a sudden increase in their gauche rotational state populations which results, on the average, in their possessing one more gauche bond than the smaller *n*-alkanes.

In an effort to determine whether or not their suggestion of a sudden conformational transition between the C_{12} and C_{14} members of the liquid *n*-alkanes has an inherent intramolecular origin, rotational isomeric state (RIS) calculations[3] are performed on isolated C_5–C_{22} *n*-alkane chains to determine the average probability $\langle P_g \rangle$ and number $\langle N_g \rangle$ of gauche bond rotations possessed by each and the probability P_g(central) that the central bond in each of the even members (C_6, C_8, C_{10}, . . . , C_{22}) is in a gauche rotational state.

The usual three-state RIS model[3] (trans and two gauche states) appropriate to *n*-alkanes and polyethylene is adopted. Each gauche rotational state incurs an energy cost of 500 cal/mol relative to the trans state and an additional 2.0 kcal/mol when it occurs paired with an adjacent gauche rotational state of the opposite sign. This RIS model has been successful in predicting the dilute solution dimensions and their temperature dependence[4] and the constant volume entropy of fusion[5] of polyethylene, the depolarized light scattering of dilute *n*-alkanes,[6] the dipole moments of the terminally substituted dibromo-*n*-alkanes[7] ($Br(CH_2-)_nBr$), and the dimensions of neat terminally halogenated *n*-alkanes.[8,9] All calculations were performed at 140 °C using the matrix multiplication methods described by Flory.[3]